arXiv:hep-ph/0302251v2 17 Sep 2003

DFCAL-TH 03/2
September 2003

Ultra-high energy neutrino-nucleon interactions

R. Fiore[a†], L.L. Jenkovszky[b‡], A. Kotikov[c⋆], F. Paccanoni[d∗], A. Papa[a†], E. Predazzi[e$]

[a] *Dipartimento di Fisica, Università della Calabria*
Istituto Nazionale di Fisica Nucleare, Gruppo collegato di Cosenza
I-87036 Arcavacata di Rende, Cosenza, Italy
[b] *Bogolyubov Institute for Theoretical Physics*
Academy of Sciences of Ukraine
UA-03143 Kiev, Ukraine
[c] *Bogolyubov Laboratory of Theoretical Physics*
Joint Institute for Nuclear Research
RU-141980 Dubna, Russia
[d] *Dipartimento di Fisica, Università di Padova*
Istituto Nazionale di Fisica Nucleare, Sezione di Padova
via F. Marzolo 8, I-35131 Padova, Italy
[e] *Dipartimento di Fisica Teorica, Università di Torino*
Istituto Nazionale di Fisica Nucleare, Sezione di Torino
via P. Giuria 1, I-10125 Torino, Italy

Abstract

Ultra-high energy ($E_\nu > 10^8$ GeV) neutrino-nucleon total cross sections $\sigma^{\nu N}$ are estimated from a soft non-perturbative model complemented by an approximate QCD evolution, explicitly calculated. The resulting asymptotic energy behavior of the neutrino-nucleon charged-current total cross section is derived analytically and predictions concerning the observation of ultra-high energy neutrinos in future experiments are presented.

[†] *e-mail address:* fiore, papa@cs.infn.it
[‡] *e-mail address:* jenk@gluk.org
[⋆] *e-mail address:* kotikov@thsun1.jinr.ru
[∗] *e-mail address:* paccanoni@pd.infn.it
[$] *e-mail address:* predazzi@to.infn.it

1 Introduction

Calculations of ultra-high energy (UHE) neutrino-nucleon cross sections $\sigma^{\nu N}$ [1, 2, 3, 4, 5, 6, 7, 8] have attracted attention for many years since, on the one hand, UHE neutrino fluxes are predicted by cosmological models but have not yet been measured experimentally and, on the other hand, theoretical models exist for the evaluation of these cross sections.

Neutrino telescopes are the most promising tools for probing the distant stars and galaxies. Due to their high stability and neutrality, neutrinos arrive at a detector on a direct line from their sources, undeflected by intervening magnetic fields, with expected energy up to 10^{20} eV. Whereas high-energy photons are completely absorbed by a few hundred grams/cm^2 of material, the interaction length of a 1 TeV neutrino is about 250 kilotonnes/cm^2 [3].

An important scientific goal of large-scale neutrino telescopes is the detection of UHE cosmic neutrinos produced outside the atmosphere, i.e. neutrinos produced by galactic cosmic rays interacting with interstellar gas, and extra-galactic neutrinos. High neutrino energy brings a number of advantages [3, 4]. Firstly, the charged-current cross section increases as $\sigma \sim E_\nu$ for $E_\nu < 10^{12}$ eV and is believed to rise as $\sigma \sim E_\nu^{0.4}$ for higher E_ν. (In this paper we question the last point.) Secondly, the background of atmospheric neutrinos decreases as compared to the flux from extra-galactic sources, approximately as $E_\nu^{-1.6}$.

Another important and promising aspect of UHE neutrino physics is the possibility to study the production of exotic objects, such as supersymmetric particles [9] or black holes [3].

The phenomenology of UHE neutrinos and their detection depend on the neutrino-nucleon total cross section, which has been calculated in the standard model (see e.g. [3]). A striking feature of these calculations is the continued power-law growth of the cross sections with E_ν at highest energies. The rise with E_ν, on the other hand, is directly related to the very low-x behavior of the nucleon parton distributions derived from e.g. the HERA data. Problems related to the unitarity bound have been discussed in [6, 10, 11, 12].

At ultra-high neutrino energies the total cross section is completely dominated by its deep inelastic component. The energy dependence of neutrino-nucleon cross section, as suggested from the small-x nucleon structure functions (SF) measured at HERA, should show a rapid increase with energy, like s^{λ} [13], where λ scales as $\ln(Q^2/\Lambda^2)$ and ranges approximately in the interval $0.1 \div 0.4$ for $1\ \mathrm{GeV}^2 < Q^2 < 100\ \mathrm{GeV}^2$ (see Ref. [14]).

The highest available ep energy at HERA, $\sqrt{s_{ep}} = 314$ GeV, is still too low as compared to the expected UHE neutrino-nucleon collision energies. For the neutrino energy $E_\nu \sim 10^{12}$ GeV, the relevant x-region is $x \sim 10^{-8}$, while the HERA measurements extend now to $x \sim 10^{-6}$; however such low values of x are measured at $Q^2 < 0.1\ \mathrm{GeV}^2$. For the interesting region of $Q^2 \sim M_W^2$, SF are measured only up to $x \sim 10^{-3}$ in the D0 experiment of inclusive jets [15]. Since studies of the UHE νN cross sections began nearly a decade ago [1, 2, 9, 16] our knowledge about quark distributions and nucleon SF improved significantly [17].

In the present paper we study the UHE behavior of the neutrino-nucleon charged-current cross section starting from models where nucleon SF have a milder increase. Our analysis relies strongly on recent progress and our previous experience in the studies of the nucleon SF [17, 18, 19, 20, 21, 22, 23], based on phenomenological fits, extended by QCD evolution.

The paper is organized as follows: in the next Section we briefly review the steps involved in the determination of the neutrino-nucleon cross section and illustrate our approach; in Section 3 we study the asymptotic behavior of the total neutrino-nucleon cross section; in Section 4 we discuss the implications of our results for the observation of UHE neutrinos in future experiments and finally in Section 5 we draw some conclusions.

2 Nucleon structure functions and neutrino-nucleon cross sections

In order to compute the cross section for neutrino-nucleon interactions at high energies, one needs a detailed description of the quark structure of the nucleon. The special challenge of the UHE neutrino-nucleon cross section is that the W-boson propagator emphasizes smaller and smaller values of x as the neutrino energy E_ν increases. In the UHE domain, the most important contribution to the νN cross section comes from $x \sim M_W^2/(2ME_\nu)$ and hence the greatest uncertainty in the predictions comes from the small-x extrapolation.

Deep inelastic scattering of UHE neutrinos is unique in the sense that it explores extreme regions of the (Q^2, x) phase space where no accelerators data exist. One thus must rely on predictions or assumptions regarding the nature of these distributions, in particular in the region of ultra-low x and low Q^2, as well as in the region of low x and low Q^2.

Let us consider the double differential cross section for the deep inelastic scattering of neutrinos on an isoscalar target for charged-current processes. We will limit ourselves to the leading order corrections to the simple parton model and hence all parton model formulas remain unchanged except that the parton distributions now depend on x and Q^2 and not only on x. In particular, the Callan-Gross relation, $F_2 = 2xF_1$ or $F_L = 0$, holds in leading order [24]. With the usual notation we can then write for charged-current neutrino interactions

$$\begin{aligned}\left(\frac{d\sigma}{dx\,dy}\right)^{\nu} &= \frac{G_F^2 M E_\nu}{\pi}\left(\frac{M_W^2}{Q^2+M_W^2}\right)^2 \\ &\times \left\{\frac{1+(1-y)^2}{2}F_2^{\nu}(x,Q^2) + \left(1-\frac{y}{2}\right) yxF_3^{\nu}(x,Q^2)\right\}. \quad (1)\end{aligned}$$

For anti-neutrino charged-current processes one must change the sign in front of $F_3^{\nu}(x,Q^2)$. (The changes necessary in order to describe neutral-current neutrino interactions are given in many textbooks and review articles, for example in [24]). In Eq. (1), G_F is the Fermi constant, M is the nucleon mass and the variable y is related to the Bjorken x through the relation

$$y = \frac{Q^2}{x(s - M^2)} \simeq \frac{Q^2}{xs} \ , \tag{2}$$

where s is the square of the c.m. energy for the neutrino-nucleon scattering. The laboratory neutrino energy $E_\nu = (s - M^2)/(2M)$ is approximately $s/(2M)$ in the energy region of interest.

The main purpose of this paper is to evaluate the asymptotic behavior of the total cross section for charged-current neutrino-nucleon process

$$\sigma^{\nu N\,(CC)} = \int_0^1 dx \int_0^1 dy \left(\frac{d\sigma}{dx\,dy}\right)^\nu \tag{3}$$

in a model for the structure function F_2 based on a soft non-perturbative input complemented by an approximate QCD evolution. The contribution of xF_3 can in fact be neglected at ultra-high energies. Unfortunately, experimental data for the neutrino SF do not extend to the “deep sea” region, i.e. to x smaller than 0.001, and to large Q^2. Both these limits, for the electromagnetic structure functions F^{ep}, are subject of debate regarding the presence of possible saturation effects at small x and discrepancies in the Q^2 evolution for large Q^2. F_2^ν differs from F_2^{ep} at small Q^2 as can be easily seen by formally integrating the double differential cross section (1) over x at fixed value of the product $(E_\nu y)$

$$\lim_{y \to 0} \frac{1}{E_\nu} \frac{d\sigma}{dy} = \frac{G_F^2 M}{\pi} \int_0^1 dx\, F_2^\nu(x, Q^2 = 0) \ , \tag{4}$$

formula that has been used for the normalization of the neutrino flux [25]. The integral in Eq. (4), when evaluated for F_2^{ep}, would vanish by gauge invariance. At increasing Q^2, this difference will disappear but, at the moment, no smooth transition has been found in all the range of the variables appearing in Eq. (3).

2.1 The non-perturbative input

In a number of papers [18, 19, 20, 21, 22, 23, 26] a diffraction model has been developed, describing equally well hadronic reactions at high energies and DIS at small x. The main idea behind the model is that SF at small and moderate values of Q^2 are Regge-behaved. The Q^2-dependence was introduced in a phenomenological way.

It was shown [18, 19, 21, 23, 26] that data on deep inelastic ep scattering from HERA and elsewhere can be fitted perfectly well by a "soft" Pomeron alone. This Pomeron could be a dipole with a $\ln(1/x)$ dependence or a squared logarithm, saturating asymptotically the Froissart bound. For the electromagnetic SF, parametrizations exist [17] that allow for a simplified evolution until very large Q^2, while maintaining a soft dependence on the Bjorken x. As an example we will consider a structure function $F_2^\nu(x,Q^2)$ of the form

$$F_2^\nu(x,Q^2) = \left[a(Q^2) + b(Q^2)\ln\left(\frac{1}{x}\right)\right](1-x)^{\nu(Q^2)} \tag{5}$$

and derive for it an explicit approximate evolution starting from $Q^2 = Q_0^2$. The main motivation for our choice of the model is that at small Q^2 there is similarity between the small-x behavior of the structure function and the s-dependence, $x \sim Q^2/s$, of the hadronic total cross section at high energies. The alternative approach, with a power behaved dependence, has been discussed in the literature in several publications. The differences between the two approaches can be significant and will be discussed in Section 3.

We notice that the coefficients $a(0)$, $b(0)$ and $\nu(0)$ are constrained by Eq. (4) whose left hand side can be determined from the experiment, Ref. [25]. The constraint is

$$\lim_{y\to 0}\frac{1}{E_\nu}\frac{d\sigma}{dy} = \frac{1}{\nu(0)+1}\Big\{a(0) + b(0)\Big(\gamma + \psi[\nu(0)+2]\Big)\Big\}\,,$$

where γ denotes the Euler's constant and $\psi[z]$ is the logarithmic derivative of the Γ-function. When low-Q^2 data [27] will extend to lower x values, it will be possible to check the choice (5).

By imposing a lower cut in Q^2, $Q^2 = Q_0^2$, and rewriting Eq. (3) as

$$\sigma^{\nu N\,(CC)} \simeq \frac{1}{2ME_\nu} \int_{Q_0^2}^{s} dQ^2 \int_{Q^2/s}^{1} \frac{dx}{x} \left(\frac{d\sigma}{dx\,dy}\right)^{\nu} ,$$

where in the differential cross section $y = Q^2/(xs)$, the F_2 contribution to the total cross section can be written in the form

$$\bar{\sigma}^{\nu N} \equiv \frac{\sigma^{\nu N} + \sigma^{\bar{\nu} N}}{2}$$

$$= \frac{G_F^2}{2\pi} \int_{Q_0^2}^{s} dQ^2 \left(\frac{M_W^2}{Q^2 + M_W^2}\right)^2 \int_{Q^2/s}^{1} \frac{dx}{x} \, \frac{1 + (1 - Q^2/(xs))^2}{2} F_2^{\nu}(x, Q^2) \ . \quad (6)$$

2.2 Q^2 evolution

Let us consider a simplified approach to the DGLAP [28] evolution, where the parton distribution functions satisfy the relation $q(x) = \bar{q}(x) = u(x) = d(x) = s(x) = 2c(x) = 2b(x)$ and F_2^{ν}, for five flavors, is given by $F_2^{\nu} = 8xq(x)$. This assumption gives $F_2^{ep} = 17xq(x)/9$ and, as shown in [16], with this simple form for the SF a high quality fit to the HERA data can be obtained.

For each parton distribution we assume the same function (5) chosen for $F_2^{\nu}(x, Q^2)$

$$xf_i(x, Q^2) = \left[a_i(Q^2) + b_i(Q^2) \ln\left(\frac{1}{x}\right)\right] (1 - x)^{\nu(Q^2)}, \quad (i = q, g) \quad (7)$$

with the same functional form for quark and gluon but with different coefficients. Experimental data for quarks and global analysis, for example the parton analysis of MRST [17], for the gluon could determine the coefficients in the expressions for $xf_i(x, Q^2)$, where $i = q, g$ stands for quark or gluon, respectively.

In the leading order of perturbation theory, an approximate evolution is feasible by using the results of Ref. [29]. The only condition is that $a_i \gg b_i$ $(i = q, g)$, where $a_i \equiv a_i(Q_0^2)$ and $b_i \equiv b_i(Q_0^2)$, so that no interference appears in the Q^2 evolution of the coefficients multiplying the different powers of the logarithm[1]. We define $\beta_0 = 11 - 2f/3$, where $f = 5$ is the number of flavors in our approach,

$$t = \ln \left[\frac{\alpha(Q_0^2)}{\alpha(Q^2)} \right] = \ln \left[\frac{\ln(Q^2/\Lambda^2)}{\ln(Q_0^2/\Lambda^2)} \right]$$

and recall the form of the scaling variables,

$$\sigma = 2\sqrt{-\hat{d}_{gg} t \, \ln(1/x)}, \qquad \rho = \sqrt{\frac{-\hat{d}_{gg} t}{\ln(1/x)}} = \frac{\sigma}{2 \ln(1/x)} \; , \tag{8}$$

where $\hat{d}_{gg} = -12/\beta_0$ [2] . Then, from [29], we get for small x the evolution of the structure function $F_2(x, Q^2) = 8x f_q(x, Q^2) = 8x[f_q^-(x, Q^2) + f_q^+(x, Q^2)]$ as

$$\begin{aligned} x f_q^-(x, Q^2) &= \left(a_q + b_q \left[\ln\left(\frac{1}{x}\right) - C_1(\nu) \right] \right) \cdot e^{-d_-(1)t} \; + O(x) & (9) \\ x f_q^+(x, Q^2) &= \left(a_q^+ \rho I_1(\sigma) + b_q^+ I_0(\sigma) \right) \cdot e^{-\bar{d}_+(1)t} \; + O(\rho), & (10) \end{aligned}$$

where $d_-(1) = 16f/(27\beta_0)$, $\bar{d}_+(1) = 1 + 20f/(27\beta_0)$, $a_q^+ = f(a_g + 4a_q/9)/9$ and an analogous expression for b_q^+. $C_1(\nu)$ is related to the logarithmic derivative of the Γ-function: $C_1(\nu) = \psi[1+\nu] - \psi[1]$. $I_0(z)$ and $I_1(z)$ are modified Bessel functions of the first kind.

We notice that the presence of higher powers of the logarithm of $1/x$ can be easily handled in this formalism provided that $a_i \gg b_i \gg \ldots$. While the evolution given by Eqs. (9)-(10) is correct in the limit of very large σ and $Q^2 \gg Q_0^2$, the requirement that the initial input must be reproduced for $Q^2 = Q_0^2$ introduces a corrective term in f_q^+ that does not affect the evolution for large Q^2. Eq. (10) should then be replaced by

$$x f_q^+(x, Q^2) = \left(a_q^+ \rho I_1(\sigma) + b_q^+ \left[I_0(\sigma) + \Delta \right] \right) \cdot e^{-\bar{d}_+(1)t} \; + O(\rho) \; , \tag{11}$$

where $\Delta = b_q C_1(\nu)/b_q^+ - 1$.

---

[1] The requirement $a_i \gg b_i$ is needed for all Q^2 values. It drastically simplifies our formulas since it avoids a mixing between a_i and b_i parameters during the Q^2 evolution.

[2] We follow here the notation of [29]: d is the ratio between the anomalous dimension and twice the QCD β-function in leading order, while $\hat{d}$ and $\bar{d}$ are, respectively, the singular and regular part of d when $n \to 1$.

3 Asymptotic behavior of $\sigma^{\nu N}$

We rewrite Eq. (6) in the form

$$\bar{\sigma}^{\nu N} = \frac{2G_F^2}{\pi} \int_{Q_0^2}^{s} dQ^2 \left(\frac{M_W^2}{Q^2 + M_W^2} \right)^2$$

$$\times \int_{Q^2/s}^{1} \frac{dx}{x} \left[1 + \left(1 - \frac{Q^2}{xs} \right)^2 \right] \left\{ x f_q^-(x, Q^2) + x f_q^+(x, Q^2) \right\} \ , \qquad (12)$$

where $xf_q^{\mp}(x, Q^2)$ are given in Eqs. (9)-(10) respectively. The integral over x can be done exactly for $f_q^-(x, Q^2)$. Let us denote this integral with the symbol $J_-(s, Q^2)$. The result is presented in Eq. (A.1) of the Appendix, and the leading behavior, for large s, of the x-integral is given by $\ln^2(s/Q^2)$.

The presence of many scales (Λ^2, Q_0^2, M_W^2 and s) makes difficult any precise estimate of the asymptotic behavior of the $xf_q^-(x, Q^2)$ contribution to $\bar{\sigma}^{\nu N}$. From the Ostrowski's inequality [30] for integrals it follows, however, that this contribution has an upper bound for $s \to \infty$:

$$\left| \int_{Q_0^2}^{s} dQ^2 \left(\frac{M_W^2}{Q^2 + M_W^2} \right)^2 J_-(s, Q^2) \right| \leq \ K \ln^2 \left(\frac{s}{Q_0^2} \right) \ , \qquad (13)$$

where K is a suitable constant.

Only the small-x evolution of $f_q^+(x, Q^2)$ is known from (10) and the condition $\rho \ll 1$ requires a cutoff at the upper limit of the x-integral. Let us call it x_M with $x_M < 1$, while the Q^2-integral has now $x_M s$ as the upper limit of integration. The first integral we meet, when considering the term with $f_q^+(x, Q^2)$, is

$$\int_{Q^2/s}^{x_M} \frac{dx}{x} \, x f_q^+(x, Q^2) = e^{-\bar{d}_+(1)t} \left(a_q^+ \mathcal{I}_1 + b_q^+ \mathcal{I}_2 \right) \qquad (14)$$

and, with the change of variable $x = \exp[-z^2/(-4\hat{d}_{gg}t)]$, the solution can be easily found. Setting $\sigma_u = 2\sqrt{-\hat{d}_{gg}t \ln(s/Q^2)}$ and $\sigma_\ell = 2\sqrt{-\hat{d}_{gg}t \ln(1/x_M)}$, we obtain:

$$\mathcal{I}_1(s, Q^2) = \int_{\sigma_\ell}^{\sigma_u} dz \, I_1(z) = I_0(\sigma_u) - I_0(\sigma_\ell) \qquad (15)$$

and

$$\mathcal{I}_2(s,Q^2) = \frac{1}{-2\hat{d}_{gg}t}\int_{\sigma_\ell}^{\sigma_u} dz\, z I_0(z) = \frac{1}{-2\hat{d}_{gg}t}\Big(\sigma_u\, I_1(\sigma_u) - \sigma_\ell\, I_1(\sigma_\ell)\Big)\ . \tag{16}$$

Other integrals, coming from powers of $Q^2/(xs)$ in Eq. (12), are $O(\rho)$ with respect to those in Eqs. (15) and (16) and it is consistent with our approximation in Eq. (10) to neglect them. The proof can be found in the Appendix.

We define now the integrals

$$\mathcal{J}_k(s) = \int_{Q_0^2}^{x_M s} dQ^2 \left(\frac{M_W^2}{Q^2+M_W^2}\right)^2 e^{-\bar{d}_+(1)t}\mathcal{I}_k(s,Q^2), \quad (k=1,2) \tag{17}$$

and notice that their large-s behavior determines completely the f_q^+ contribution to the mean total cross section in this limit. Of the two integrals $\mathcal{J}_1(s)$, $\mathcal{J}_2(s)$ only the first one needs to be evaluated explicitly since

$$\frac{d\mathcal{J}_2(s)}{d\ln s} = \mathcal{J}_1(s) + O\left(\frac{1}{\ln s}\right)\ .$$

We consider then the integral $\mathcal{J}_1(s)$. The function under the integral sign in $\mathcal{J}_1(s)$ vanishes at both integration limits and has a bell-shaped form with a well defined maximum. The maximum moves at larger values of Q^2, when s increases, and its position is defined, in the limit $s\to\infty$, by the solution of the transcendental equation

$$\beta_0\alpha_s(Q_0^2)\ln(s/Q^2) - \sqrt{\frac{t\ln(s/Q^2)}{-\hat{d}_{gg}}} \times \left(\frac{8\pi Q^2}{M_W^2+Q^2}e^t + \beta_0\alpha_s(Q_0^2)\bar{d}_+(1)\right) - 4\pi e^t = 0\ , \tag{18}$$

where the variable t has been rewritten as

$$t = \ln\left[1 + \frac{\beta_0\alpha_s(Q_0^2)}{4\pi}\,\ln(Q^2/Q_0^2)\right]\ .$$

Eq. (18) can be solved for $\ln(s/Q^2)$, obtaining an explicit expression for s as a complicated function of the value of Q^2 at the maximum $Q^2_{\max}$. If we rewrite Eq. (18) as $f(s, Q^2) = 0$, we get the slope

$$\frac{dQ^2_{\rm max}}{ds} = - \left. \frac{\frac{df(s,Q^2)}{ds}}{\frac{df(s,Q^2)}{dQ^2}} \right|_{Q^2=Q^2_{\rm max}}$$

that, as can be easily shown, vanishes when $s \to \infty$.

In order to estimate the position of the maximum as a function of s, in the range 10^7 GeV $\leq s \leq 10^{15}$ GeV, we have chosen the parameters in intervals that include their most probable value and found that the position of the maximum can be roughly reproduced by a term linear in $(\ln s)^{1.5}$, while the value of the integrand, at the maximum, is near the value of the Bessel function there. The width at half height of the peak goes like $\ln s$. By multiplying the value, at the maximum, of the integrand in $\mathcal{J}_1(s)$ by the width of the peak, we get the right order of magnitude for the corresponding integral in Eq. (17), as can be verified by a numerical computation. In this limit the mass of the W-boson plays little role since $Q^2_{\rm max} \ll M_W^2$ until $s \approx 10^{15}$ GeV^2. It is then possible to conclude that, in this approach, the total cross section for neutrino-nucleon scattering increases with s faster than any power of $\ln s$ but slower than any power of s.

Most of the existing models of F_2 assume a fast, power-like increase in $1/x$ that transforms in a like increase of $\sigma^{\nu N}(E)$ [1, 2, 3, 4, 5, 6, 7, 16, 31]. In an alternative approach [18, 19, 20, 21, 22, 23, 32] the HERA data are shown to fit a model of the SF, at low and intermediate Q^2 with a moderate, logarithmic, increase in $1/x$, the observed "HERA effect" being attributed to the decrease of the non-leading contributions, relevant at larger x. DGLAP evolution transforms the logarithmic behavior in the way we have shown in Eqs. (9)-(10). It is important, however, to realize that this asymptotic behavior is quite different from the one obtained starting with a power, $x^{-\mu}$. According to [16, 29, 33], if the starting distributions have a power-law form in x, the leading term keeps the same x-dependence under DGLAP evolution also at the next-to-leading order. The component $xf_q^+(x, Q^2)$ in Eq. (10) can be represented, in the leading order of perturbation theory and in the small-x

limit, by the approximated form [33, 34]

$$xf_q^+(x,Q^2) \simeq \frac{f}{9}\mu\, xf_g(x,Q_0^2)e^{-d^+t} \;, \tag{19}$$

if $xf_i(x,Q_0^2) = h_i(Q_0^2)x^{-\mu}, \quad (i = q,g)$. In Eq. (19), $d^+ = \gamma^+/(2\beta_0)$ is the largest eigenvalue of the anomalous dimension matrix evaluated at $(1+\mu)$. [3] For $\mu \sim 0.4$, as in Ref. [16], d^+ is negative and $d^+ \approx -3.4$. In this approach it is easy to show that $\bar{\sigma}^{\nu N} \propto (s/M_W^2)^\mu + O(s^0)$.

It is interesting to compare our result based on Eqs. (15) and (16) with a model where the cross section increases like a power of s [3]. We notice that Eq. (12) can be written as

$$\bar{\sigma}^{\nu N} \approx \frac{4G_F^2}{\pi}\left(a_q^+\mathcal{J}_1 + b_q^+\mathcal{J}_2\right) \tag{20}$$

and that all the integrals can be evaluated numerically, choosing for example $Q_0^2 = 10$ GeV^2, $\alpha_s(Q_0^2) = 0.23$ and the values $x_M = 0.001, 0.01$. The choice of $Q_0^2 = 10$ GeV^2 is reasonable because in the region of Q^2 near this value the rise in x of SF is well described by a $\ln(1/x)$ and/or $\ln^2(1/x)$ behavior [4].

By evaluating the integrals numerically, a comparison can be done with the values of $\bar{\sigma}^{\nu N}$ obtained from Table I of Ref. [3]. We plot in Fig. 1 the values of $P_i \equiv (4G_F^2/\pi)\mathcal{J}_i$ and the result of Ref. [3]. As can be seen from Fig. 1, the power-behaved cross section increases with s faster than the components of $\bar{\sigma}^{\nu N}$ in the relation (20). The explicit values of the parameters a_q^+ and b_q^+ do not enter this comparison, but it turns out that their order of magnitude can be made consistent with the parametrizations of the HERA data studied in Ref. [21].

---

[3] Note that the power-like behavior $\sim x^{-\hat{d}_{gg}t}$ of parton distributions is in agreement also with the DGLAP dynamics in the Q^2 range near the starting point Q_0^2 (see Refs. [35, 34]). However, the power-like behavior cannot be combined together with (19) to some unified Regge-like Q^2-evolution of parton distributions.

[4] For larger Q^2 values, the rise of F_2 is stronger and is better described by a power law $x^{-\lambda}$, with $\lambda \sim 0.3$ at $Q^2 \sim 100$ GeV^2. Evidently, our initial conditions (7) cannot be applied here. However, after Q^2 evolution in our approach, we get a behavior with a Q^2-dependent effective slope $\lambda_{\rm eff}(Q^2)$ in agreement with experimental data [14].

The Bessel-like asymptotic behavior of the total cross section in Eq. (20) violates the Froissart bound since it is steeper than any power of $\ln s$, though being flatter than any power of s. The comparison with a power-behaved cross section, strongly violating the Froissart bound, makes us confident on the fact that additional contributions needed to restore unitarity should be less relevant in our approach.

4 Observation of ultra-high energy neutrinos

The evolution in leading order considered in the present paper overestimates the cross sections. Next-to-leading calculations show (see, for example, Ref. [8]) that the ratio $\sigma_{\rm NLO}/\sigma_{\rm LO}$ decreases when the neutrino energy increases and it is reasonable to assume that our estimates constitute an upper bound for the true predictions of the model. Hence the NLO evolution of the soft non-perturbative input could lead to a more pronounced difference in the predictions with respect to a power-like input. Another possible cause for the decrease of the true cross sections, that has not been taken into account here, resides in the gluon recombination at small x. [5] This recombination can be mimicked by considering a large, "effective" gluon anomalous dimension, with a consequent increase of the value of $\bar{d}_+(1)$ that appears in the exponential $\exp(-\bar{d}_+(1)\,t)$ in Eq. (10). Despite these possible corrections, it is of interest to consider the constraints imposed by our model on the interaction length of neutrinos and compare them with a more conventional approach.

For this purpose, we considered the (water equivalent) interaction length, defined as

$$L_{\rm int}(E_\nu) = \frac{1}{\sigma^{\nu N}(E_\nu) N_A} \ ,$$

where $N_A = 6.022 \times 10^{23}$ cm^{-3} (water equivalent) is the Avogadro's number, and evaluated the ratio of $L_{\rm int}(E_\nu)$ to $L_{\rm int}(10^8$ GeV) as obtained from our model, with b_q^+/a_q^+ ranging between 1/20 and 1/3 and setting $Q_0^2 = 10$ GeV^2, $\alpha_s(Q_0^2) = 0.23$ and $x_M = 0.01$. In Fig. 2 our result is compared with the same ratio determined from the results of Ref. [3]. At higher energies L_{int} in our model could be larger than expected in more conventional approaches.

---

[5] The results of numerous analyses of the higher-twist contributions in DIS [36] and of recent papers discussing screening effects in neutrino-nucleon cross-section [11, 12] are still not conclusive.

Experiments are planned to detect UHE neutrinos by observation of the nearly horizontal air showers (HAS) in Earth atmosphere resulting from ν-air interactions. The expected rates are proportional to the neutrino-nucleon cross section. The resulting cross section at 10^{20} eV is rather high, $\sim 10^{-31}$ cm^2 according to the estimates of [16, 3], and results from the extrapolation of parton distribution functions far beyond the reach of experimental data.

If the cross section is lower, then the event rate for neutrino-induced HAS is reduced by the same factor. This reduction would compromise the main detection signal that has been proposed for UHE neutrino experiments. A smaller cross section would however offer a double advantage for the planned experiments [4]:

1. with a new search strategy, based on the observation of upgoing air showers (UAS) initiated by muon and tau leptons produced by neutrinos interacting just below the surface of Earth, the neutrino event rate with a small cross section is actually larger than the HAS rate with a large cross section;

2. the future detectors can also measure the neutrino cross section at energies far beyond those achievable in collider experiments thus providing important information for particle physics.

If the proposed model is correct, the above scenario may have better chances to be realized.

5 Conclusions

UHE neutrinos became an extremely rich and interesting testing field for various physical phenomena, such as cosmology, astrophysics (origin of UHE neutrinos), theory of gravitation (production of black holes), unified theories, testing the standard theory and beyond, as well as the strong interaction theory, responsible for the hadron structure. We predict that the UHE neutrino cross sections rise moderately with energy, in accord with the above-mentioned “soft” Pomeron dynamics.

In the present paper we concentrated on the calculation of the asymptotic behavior of the structure functions and resulting cross sections. We are aware, however, about the important role of the large and intermediate x behavior of the structure functions to be fitted to the existing, relatively low-energy, data. The cross sections calculated in this way should match with their UHE asymptotic behavior. We intend to address this point in a forthcoming publication.

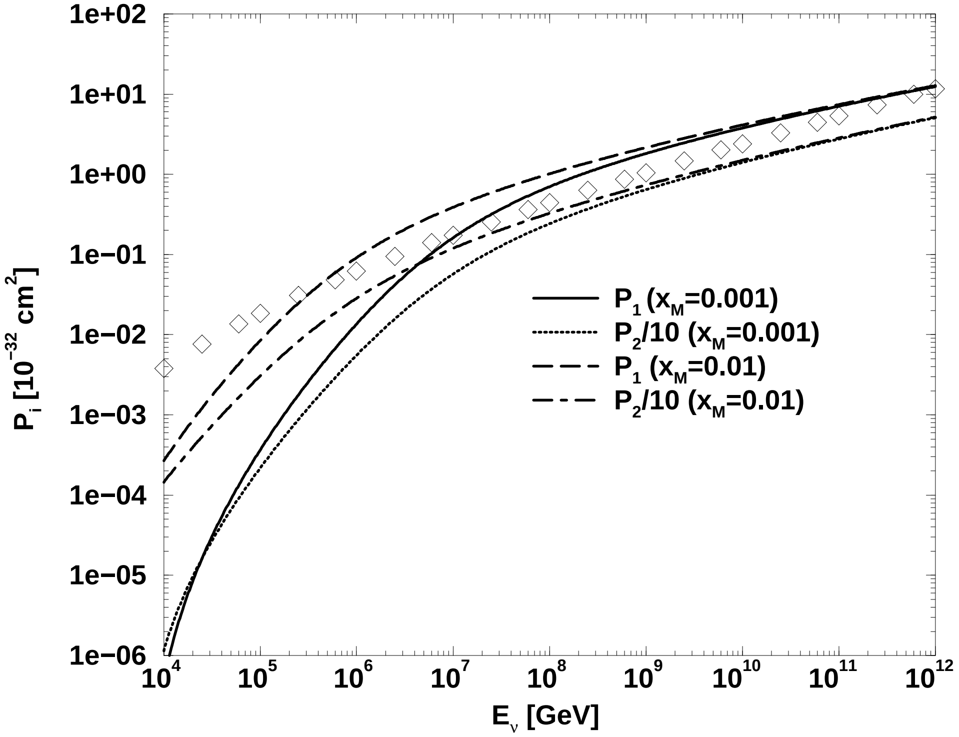

Figure 1: The curves of P_1 (solid for $x_M = 0.001$, dashed $x_M = 0.01$) and $P_2/10$ (dotted for $x_M = 0.001$, dot-dashed for $x_M = 0.01$) are plotted versus the neutrino energy E_ν together with data for $\bar{\sigma}^{\nu N}$ (diamonds) from Ref. [3].

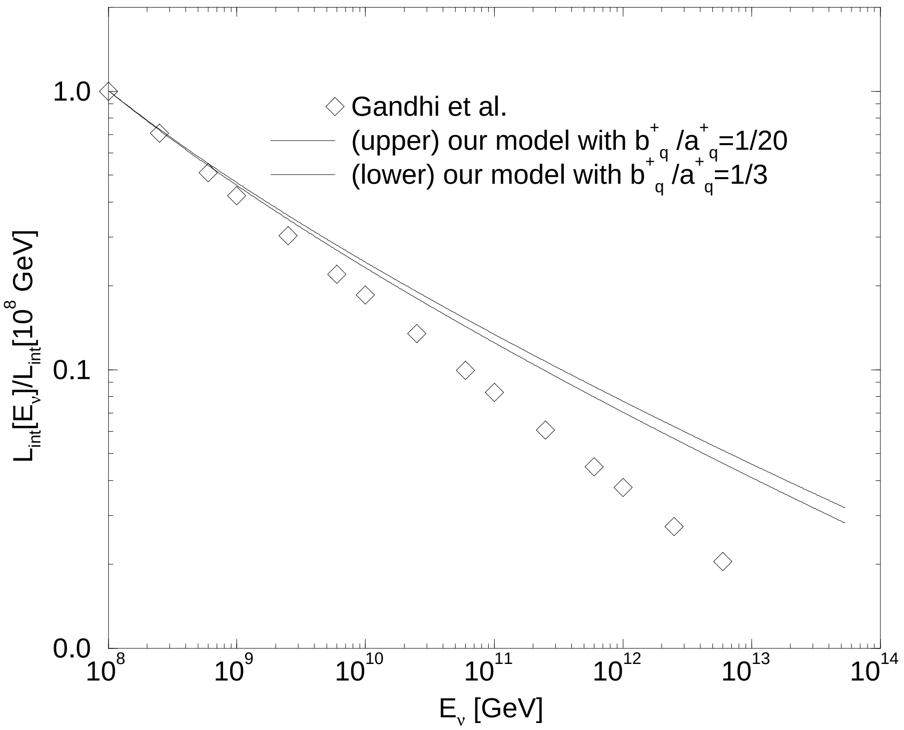

Figure 2: $L_{\rm int}(E_\nu)/L_{\rm int}(10^8\ {\rm GeV})$ versus E_ν in our model (solid lines) and according to the results of Ref. [3] (diamonds).

A Appendix

In this Appendix we include formulas that are not strictly necessary to understand the logical lines in the main text, but can be useful in reproducing some relevant results.

In order to determine the asymptotic behavior of $\sigma^{\nu N}$ we needed some cumbersome integrals and the first one is

$$\begin{aligned} J_-(s,Q^2) = \int_{Q^2/s}^1 \frac{dx}{x}\left[1+\left(1-\frac{Q^2}{xs}\right)^2\right] x f_q^-(x,Q^2) \\ = \frac{1}{2}e^{-d_-(1)t}\left\{-3a_q+\left(3C_1(\nu)+\frac{7}{2}\right)b_q+\frac{4Q^2}{s}[a_q-(C_1(\nu)+1)b_q]\right. \\ + \frac{Q^4}{s^2}\left[-a_q+\left(C_1(\nu)+\frac{1}{2}\right)b_q\right]+4\ln\left(\frac{s}{Q^2}\right)\left[a_q-\left(C_1(\nu)+\frac{3}{4}\right)b_q\right] \\ \left. + 2\ln^2\left(\frac{s}{Q^2}\right)b_q\right\} \ . \end{aligned} \tag{A.1}$$

Next, we prove that the integral

$$\frac{Q^2}{s}\int_{Q^2/s}^{x_M}\frac{dx}{x^2}\rho I_1(\sigma) \tag{A.2}$$

is non-leading, $O(\rho)$, with respect to the integral evaluated in Eq. (15). The identity

$$\frac{d}{dx}\left[\rho^n I_n(\sigma)\right] = -\frac{1}{x}\,\rho^{n+1}I_{n+1}(\sigma), \quad n=0,1,2,\ldots \tag{A.3}$$

can be easily obtained by using the definitions (8). Integrating repeatedly by part, we get

$$\begin{aligned} \int \frac{dx}{x^2}\rho I_1(\sigma) = -\frac{1}{x}\rho I_1(\sigma) - \int \frac{dx}{x^2}\rho^2 I_2(\sigma) = \\ = \frac{1}{x}\sum_{k=1}^{\infty}(-1)^k\rho^k I_k(\sigma) \ . \end{aligned} \tag{A.4}$$

The dominant contribution to the integral (A.2) comes from the lower limit of integration and, since the z asymptotics of $I_k(z)$ does not depend on k, we get

$$\frac{Q^2}{s}\int_{Q^2/s}^{x_M}\frac{dx}{x^2}\rho I_1(\sigma)\approx\left(1+O(1/\sqrt{\ln s})\right)[\rho I_1(\sigma)]_{x=Q^2/s}$$

that is non-leading with respect to the integral in Eq. (15). By using the same arguments, it is easy to show that

$$\frac{Q^4}{s^2}\int_{Q^2/s}^{x_M}\frac{dx}{x^4}\rho I_1(\sigma)\approx\frac{1}{2}\left(1+O(1/\sqrt{\ln s})\right)[\rho I_1(\sigma)]_{x=Q^2/s}\ .$$

Acknowledgments L.J. thanks the Dipartimento di Fisica Teorica dell'Università di Torino, the Dipartimento di Fisica dell'Università della Calabria and the Dipartimento di Fisica dell'Università di Padova, together with the Istituto Nazionale di Fisica Nucleare (INFN), Sezioni di Padova e Torino e Gruppo collegato di Cosenza, where this work was done, for their warm hospitality and financial support. A.K. thanks for the same the Dipartimento di Fisica dell'Università di Padova and the INFN Sezione di Padova; he is supported by the INFN-LThPh agreement program. L.J. thanks A. Kusenko for an inspiring correspondence.

References

[1] Yu.M. Andreev et al., Phys. Lett. B **84** (1979) 247.

[2] D.W. McKay and J.P. Ralston, Phys. Lett. B **167** (1986) 103.

[3] R. Gandhi et al., Phys. Rev. D **58** (1998) 093009; Astropart. Phys. **5** (1996) 81.

[4] A. Kusenko and T.J. Weiler, Phys. Rev. Lett. **88** (2002) 161101; A. Kusenko, `hep-ph/0203002`.

[5] J. Kwiecinski, A.D. Martin and A.M. Stasto, Phys. Rev. D **59** (1999) 093002.

[6] M. Reno et al., `hep-ph/0110235`.

[7] M. Gluck et al., Astropart. Phys. **11** (1999) 327.

[8] R. Basu et al., JHEP **10** (2002) 012.

[9] A.V. Butkevich et al., Zeit. Phys. C **39** (1988) 241.

[10] D.A. Dicus et al., Phys. Lett. B **514** (2001) 103.

[11] K. Kutak and J. Kwiecinski, hep-ph/0303209.

[12] J. Jalilian-Marian, hep-ph/0301238.

[13] E.A. Kuraev, L.N. Lipatov and V.S. Fadin, Sov. Phys. JETP **45** (1977) 199; Ya.Ya. Balitsky and L.N. Lipatov, Sov. J. Nucl. Phys. **28** (1978) 822 and Sov. Phys. JETP **63** (1986) 904.

[14] H1 Collab., C. Adloff et al., Phys. Lett. B **520** (2001) 183.

[15] L. Babukhadia (D0 Collab.), `hep-ex/0106069`.

[16] G.M. Frichter, D.W. McKay and J.P. Ralston, Phys. Rev. Lett. **74** (1995) 1508.

[17] A.D. Martin et al., Eur. Phys. J. C **23** (2002) 73; `hep-ph/0211080`; S.I. Alekhin, Phys. Rev. D **63** (2001) 094022; V.G. Krivokhijine and A.V. Kotikov, `hep-ph/0108224`.

[18] L. Jenkovszky, F. Paccanoni and E. Predazzi, Nucl. Phys. B (Proc. Suppl.) **25** (1992) 80.

[19] P. Desgrolard et al., Phys. Lett. B **309** (1993) 191.

[20] M. Bertini et al., Rivista Nuovo Cimento **19** (1996) 1.

[21] P. Desgrolard et al., Phys. Lett. B **459** (1999) 265.

[22] L. Csernai et al., Eur. Phys. J. C **24** (2002) 205.

[23] L. Jenkovszky, A. Lengyel and F. Paccanoni, Nuovo Cim. A **111** (1998) 551.

[24] A. Buras, Rev. Mod. Phys. **52** (1980) 199.

[25] E. Oltman et al., Zeit. Phys. C **53** (1992) 51.

[26] R. Fiore, L.L. Jenkovszky, E.A. Kuraev, A.I. Lengyel, F. Paccanoni and A. Papa, Phys. Rev. D **63** (2001) 056010; R. Fiore, L.L. Jenkovszky, F. Paccanoni and A. Papa, Phys. Rev. D **65** (2002) 077505.

[27] B.T. Fleming et al. (CCFR/NuTev Coll.), Phys. Rev. Lett. **86** (2001) 5430.

[28] G. Altarelli and G. Parisi, Nucl. Phys. B **126** (1977) 298; V.N. Gribov and L.N. Lipatov, Yad. Fiz. **15** (1972) 781 [Sov. J. Nucl. Phys. **15** (1972) 438]; L.N. Lipatov, Yad. Fiz. **20** (1974) 181 [Sov. J. Nucl. Phys. **20** (1974) 94]; Yu. L. Dokshitzer, Zh. Eksp. Teor. Fiz. **73** (1977) 1216 [Sov. Phys. JETP **46** (1977) 641].

[29] A.V. Kotikov and G. Parente, Nucl. Phys. B **549** (1999) 242.

[30] I.S. Gradshteyn and I.M. Ryzhik, *Tables of Integrals, Series, and Products*, Academic Press.

[31] A.Z. Gazizov and S.I. Yanush, Phys. Rev. D **65** (2002) 093003, `astro-ph/0112244`, `astro-ph/0201528`.

[32] A. De Roeck and E.A. De Wolf, Phys. Lett. B **388** (1996) 843.

[33] A.V. Kotikov, Phys. Rev. D **49** (1994) 5746; Phys. Atom. Nucl. **57** (1994) 133.

[34] A.V. Kotikov, Mod. Phys. Lett. A **11** (1996) 103; Phys. Atom. Nucl. **59** (1996) 2137.

[35] L.L. Jenkovszky, A.V. Kotikov and F. Paccanoni, Sov. J. Nucl. Phys. **55** (1992) 1224; Phys. Lett. **B314** (1993) 421.

[36] L.V. Gribov, E.M. Levin and M.G. Ryskin, Phys. Rep. **100** (1983) 1; A.H. Mueller and J. Qiu, Nucl. Phys. B **268** (1986) 427; L. McLerran and R. Venugopalan, Phys. Rev. D **49** (1994) 2233, D **49** (1994) 3352, D50 (1994) 2225; Y.V. Kovchegov, Phys. Rev D **60** (1999) 034008; W. Zhu and J. Ruan, Nucl. Phys. B **559** (1999) 378; J. Blümlein et al., Phys. Lett. B **504** (2001) 235.